Structure of energy-level degeneracy of a single-spin model from a viewpoint of symmetry of the spin anisotropy and its nontrivial spin dependence on the higher-order anisotropy

Keigo Hijii[1,2] and Seiji Miyashita[1,2]
[1]*Department of Physics, Graduate School of Science, University of Tokyo, Bunkyo-ku, Tokyo 113-0033, Japan*
[2]*CREST, JST, 4-1-8 Honcho, Kawaguchi, Saitama 332-0012, Japan*

(Received 4 October 2008; revised manuscript received 4 December 2008; published 30 December 2008)

We study structure of the gapless points (diabolical points) at zero magnetic field ($H_z=0$) of single-spin models with spin anisotropies. Nontrivial appearance of diabolical points at finite transverse field H_x has been studied from the viewpoint of interference of the Berry phase and related phenomena have been experimentally found in the single molecular magnet Fe_8. We study effects of the orthorhombic single-ion anisotropy $E(S_+^2+S_-^2)$ and find a symmetry associated with the degeneracy, which provides a clear picture of the global structure of energy-level diagram including the excited states. Moreover, we study effects of the higher-order anisotropy $C(S_+^4+S_-^4)$ and find that, in contrast to the semiclassical limit ($S\to\infty$), location of a pair annihilation of the diabolical point does not coincide with a point at which a pair of diabolical points appears in nonzero H_y space (bifurcation points). Distance between the annihilation and bifurcation points vanishes when $S\to\infty$, which restores the semiclassical result. We obtain a complete structure of the diabolical points in the (C,H_x) plane.

DOI: 10.1103/PhysRevB.78.214434 PACS number(s): 75.10.Jm, 75.45.+j, 75.75.+a, 75.30.Gw

I. INTRODUCTION

Single molecular magnets, e.g., Mn_{12}, Fe_8, and V_{15}, are interesting objects from both theoretical and experimental points of view in physics and chemistry.[1–5] Because those molecules consist of small number of magnetic atoms, the energy levels are discrete. There, we observe characteristics due to quantum-mechanical motion of the wave function. In particular, in the high-spin molecular magnets with an easy-axis anisotropy, such as Mn_{12} and Fe_8, a steplike magnetization process where M_z suddenly changes has been observed in a sweep of the magnetic field. This phenomenon is understood to be attributed to the quantum tunneling between two values of M_z and is called resonant tunneling.[6–11] The energy-level diagram as a function of the magnetic field H_z consists of linear lines denoting the Zeeman energy (diabatic state). At the crossing point of the energy levels, however, they form an avoided level-crossing structure due to some quantum mixing interactions which cause nonzero matrix element between the crossing states. When the field crosses these points, the state undergoes adiabatic and nonadiabatic transitions. This quantum-mechanical aspect of magnetization process has been studied from the viewpoint of Landau-Zener-Stueckelberg mechanism.[12–15] There, the energy gap and sweeping velocity determine properties of the transition. By making use of this formula, determinations of the energy gaps have been performed.[16–18] Besides the high-spin molecules, there have been found also various types of magnetization processes which reflect the quantum-mechanical aspects of specific energy-level diagram of the systems.[19–23] These systems have attracted attentions also from viewpoints of possible applications, for example, a basic component of a quantum computer.[24]

The energy gap is understood as a tunnel splitting of the energy levels. That is, by tunneling between classically degenerate minima of a potential, the degeneracy is broken. The idea of quantum tunneling of magnetization was proposed by Bean and Livington[25] and the first theoretical description was given by Chudnovsky.[26] This tunneling phenomenon can be characterized by the instanton solution in the semiclassical treatments.[27–29] Thus, usually the ground state in finite quantum systems is unique.

However, in some situation, a degeneracy can exist as predicted by Bogachek and Krive.[30] The point at which the energy gap vanishes is called a "diabolical point."[31] It was pointed out that an interference of Berry phase[32] plays an important role in small magnetic particles.[33–35] Garg[36] studied this phenomenon by studying destructive interference of the Berry phase by using the spin coherent-state path-integral formulation. He showed that the tunnel splitting at $H_z=0$ is quenched in a single-spin system of a large spin S with biaxial anisotropy of the terms $[-DS_z^2+E(S_+^2+S_-^2)]$ under nonzero transverse fields H_x (Refs. 36 and 37) even when Kramers' theorem is inapplicable. There, the tunnel splitting is found to oscillate as a function of the transverse field. That is, energy gaps vanish at some values of the transverse field H_x. Villain and Fort[38] studied a case of large spin in a weak external field limit. They rederived Garg's result and extended the study in the (H_x,H_z) plane. Keçecioğlu and Garg[39] obtained exact locations of diabolical points algebraically in a model Hamiltonian.

Werensdorfer and Sessoli[18] experimentally observed the oscillating behavior of tunnel splitting in the molecular magnet $[Fe_8O_2(OH)_{12}(tacn)_6]^{8+}$ (called Fe_8). This spin system consists of eight Fe atoms, each of which has $S=5/2$ conforming a ferrimagnetic structure. The ground state of this molecule has the total spin $S=10$.[40] This material is well described by a single large spin model. They measured tunnel splitting of this material using the Landau-Zener-Stueckelberg theory. There, it is found that the number of diabolical points is smaller than that expected from S, which is called "the missing paradox."

Effects of the higher-order anisotropy $C(S_+^4+S_-^4)$ are also studied. Keçecioğlu and Garg explained the missing paradox

as an effect of the higher-order anisotropy.[41,42] Bruno[43] pointed out a pair annihilation of diabolical points in the (C,H_x) plane and they move to the nonzero H_y space. They discussed the case with the large S limit using spin coherent-state path-integral formulation.

In the present paper, we point out that the mechanism of degeneracy at finite values of H_x can be understood from a view of a kind of parity effect in the eigenvalues of S_x which is directly obtained from the symmetry of the Hamiltonian of the system. This symmetry argument provides a clear picture of the global structure of energy-level diagram including the excited states.

Moreover, we study the effects of the higher-order anisotropy $C(S_+^4+S_-^4)$ on positions of diabolical points in the (C,H_x) plane and determine a complete structure of diabolical points in the plane. There, we find three types of pair annihilation of the diabolical points and also find out to where the diabolical points move from the plane. It should be noted that in the case of finite S, the pair annihilation point at finite H_x does not coincide with the point where a pair of diabolical points appears in nonzero H_y space (bifurcation point) in contrast to the semiclassical case $(S\to\infty)$.[43] We find that the distance between the annihilation and bifurcation points vanishes when $S\to\infty$, Namely, the semiclassical result is restored in this limit. We also study a difference in the structure of diabolical points for odd and even values of S, which should be related to the parity effect pointed in the literature.[6]

This paper is organized as follows. In Sec. II, we introduce a single-spin model of single molecular magnets. In Sec. III, we study symmetry of the Hamiltonian of the single-spin model in relation to the nontrivial degeneracy. In Sec. IV, we discuss the effects of the higher-order anisotropy. Finally, in Sec. V, we summarize the present results.

II. MODEL

In this paper, we study structures of energy-level diagram of a large spin model described by

$$\mathcal{H}=-DS_z^2+E(S_+^2+S_-^2)+C(S_+^4+S_-^4)-\boldsymbol{H}\cdot\boldsymbol{S}, \tag{1}$$

where $\boldsymbol{S}$ is a spin operator with three components (S_x,S_y,S_z), and $\boldsymbol{H}$ is an external magnetic field (H_x,H_y,H_z). The terms of D, E, and C represent the single-ion anisotropies. When D and $E(<D)$ are positive, the easiest axis is the z axis $(-DS_z^2)$ and the hardest axis is the x axis $(2ES_x^2)$. This large spin model is used to study properties of single molecular magnets such as Mn_{12} and Fe_8. For these molecules, the total spin S of the ground state can be regarded to be $S=10$.[40,44]

In particular, we study effects of the system parameters on the energy levels and discuss the behavior of the diabolical points, at which the ground state is degenerate at $H_z=0$ as mentioned in Sec. I. Throughout the paper, we take D as a unit of energy $(D=1)$.

III. SYMMETRY OF THE MODEL WITH BIAXIAL ANISOTROPY UNDER AN EXTERNAL FIELD H_x

A. Special symmetric point

As mentioned in Sec. I, the problem of the diabolical point has been studied extensively for the model (1). There, the ground-state degeneracy at $H_z=0$ is studied as a function of H_x and found that the energy gap disappears at certain values of H_x. Generally, disappearance of the gap is associated with existence of a kind of symmetry. So far, the symmetry of the model has been discussed in the path-integral formulation, where the gap disappearance is attributed to a destructive interference of the Berry phase.

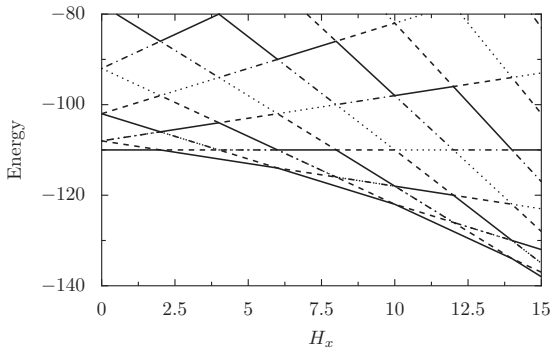

FIG. 1. Energy diagram of the low-lying levels of the system (1) with $S=10$ as a function of the field H_x for $E=0.5$.

In this section, we study the symmetry of the model (1) with $C=0$ and the magnetic field along x axis,

$$\mathcal{H}=-DS_z^2+E(S_+^2+S_-^2)-H_xS_x, \tag{2}$$

from a viewpoint of explicit form of the Hamiltonian consisting of spin operators.

Because we consider the case that the principal anisotropy axis is along the z axis, naively, we consider that the existence of H_x destroys the symmetry of the Hamiltonian. However, it should be noted that at a certain combination of D and E, i.e.,

$$E=0.5D, \tag{3}$$

the Hamiltonian can be expressed as follows:

$$\mathcal{H}_0=-DS_z^2+D(S_x^2-S_y^2)-H_xS_x=2DS_x^2-H_xS_x-DS(S+1). \tag{4}$$

This Hamiltonian only consists of S_x and thus it is commutative with S_x. Therefore, this Hamiltonian can be diagonalized simultaneously with S_x, where the eigenstates are

$$S_x|M_x\rangle=M_x|M_x\rangle, \quad M_x=-S,-S+1,\ldots,S. \tag{5}$$

In this system, the energy levels are linear as a function of H_x and cross each other without gap. Because D is positive, at $H_x=0$ the ground state is a state of $M_x=0$, i.e., $|M_x=0\rangle$; for $S=10$, the ground-state energy is $-110D$. The first-excited state is degenerate and they have $M_x=\pm 1$. When we increase H_x, the ground state is replaced by a state with a larger magnetization M_x+1 sequentially. That is, at $H_x=2$, the energy level of state $|M_x=1\rangle$ crosses with that of $|M_x=0\rangle$, then $|M_x=1\rangle$ becomes the ground state. Similarly, the ground-state magnetization changes to $M_x=2,3,\ldots$ at $H_x=6,10,\ldots$, respectively. In Fig. 1, we depict the energy diagram of the model of Eq. (2) as a function of the field H_x. In Fig. 2, we plot the energy gap between the ground-state energy (E_G) and the first-excited energy (E_1),

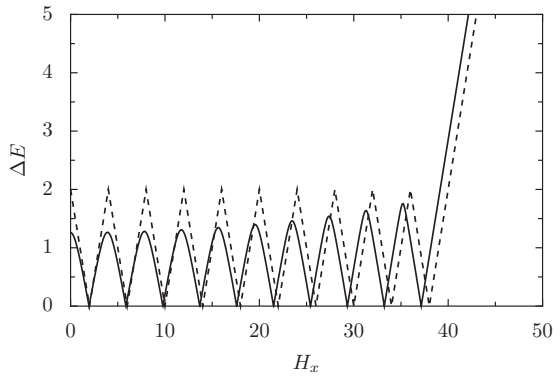

FIG. 2. Energy gap between the lowest energy and the first-excited energy of the system (2) with $S=10$ as a function of the transverse field H_x. The solid line is the case of $E=0.485$; the dashed line is the case of $E=0.5$.

$$\Delta E = E_1 - E_G, \tag{6}$$

by dashed lines as a function of H_x. There, we see a sawtooth shape as shown.

B. General biaxial anisotropy

Next, we consider the case with $E \neq 0.5D$. We set

$$E = 0.5D + \Delta. \tag{7}$$

The Hamiltonian becomes

$$\mathcal{H} = \mathcal{H}_0 + \mathcal{H}', \tag{8}$$

with

$$\mathcal{H}' = \Delta(S_+^2 + S_-^2) = 2\Delta(S_x^2 - S_y^2). \tag{9}$$

Here, the states $|M_x\rangle$ are no more the eigenstates of the Hamiltonian $\mathcal{H}$. The effects of the term S_y^2 are expressed in terms of the raising (S_x^+) and lowering (S_x^-) operators of for M_x as

$$S_y^2 = \left[\frac{1}{2}(S_x^+ + S_x^-)\right]^2 = \frac{1}{4}(S_x^{+2} + S_x^+ S_x^- + S_x^- S_x^+ + S_x^{-2}). \tag{10}$$

This term causes the change of M_x by 2. The explicit matrix element of this operator is $\langle M_x{=}m|S_y^2|M_x{=}n\rangle$,

$$\begin{aligned} &= \frac{1}{4}[S(S+1) - n(n+1)]^{1/2}[S(S+1) \\ &- (n+1)(n+2)]^{1/2}\delta_{m,n+2} \\ &+ \frac{1}{4}[2S(S+1) - 2n^2]\delta_{m,n} \\ &+ \frac{1}{4}[S(S+1) - n(n-1)]^{1/2}[S(S+1) \\ &- (n-1)(n-2)]^{1/2}\delta_{m,n-2}. \end{aligned} \tag{11}$$

This term mixes the eigenstates $|M_x{=}m\rangle$ and $|M_x{=}n\rangle$ when

$$|m-n| = 2, \tag{12}$$

and thus it opens a gap in the crossing points with even values of $|m-n|$ in the energy diagram in Fig. 1. In contrast,

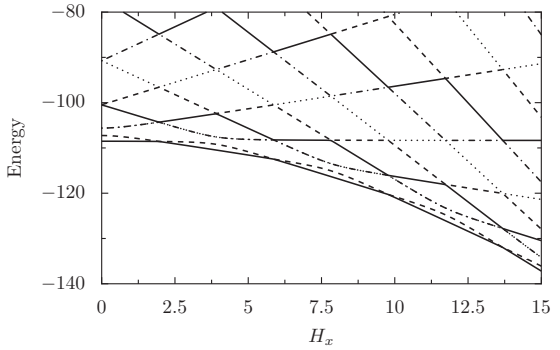

FIG. 3. A ribbonlike structure of energy diagram of the low-lying levels of the system (2) with $S=10$ and $E=0.485$ as functions of the field H_x.

it does not open a gap between $|M_x{=}m\rangle$ and $|M_x{=}m\pm1\rangle$ because

$$\langle M_x = m|S_y^2|M_x = m \pm 1\rangle = 0, \tag{13}$$

and

$$\langle M_x = m|S_y^2|M_x = n\rangle\langle M_x = n|S_y^2|M_x = m \pm 1\rangle = 0 \tag{14}$$

for all the possible integer values of n.

Therefore, when the difference of the magnetization M_x between the ground state and the first-excited state is one, the cross points in Fig. 1 remain gapless points ($\Delta E=0$). On the other hand, those of the difference two change to avoided level crossings. By this effect of S_y^2, the energy diagram has a ribbonlike shape as depicted in Fig. 3, and the H_x dependence of the gap is smoothed as depicted in Fig. 2 by a solid curve. It should be noted that the value of E/D is 0.082 for Fe_8 and is much smaller for Mn_{12}. Here we used a large value of E/D just because of the convenience for drawing the figure. If we use a small value of E/D, the energy difference is too small to see. The physical mechanism is the same irrespective of the value and here we use a large value. If we decrease the value of E down to $E=0.3$, the ground state and the first-excited state almost degenerate as depicted in Fig. 4.

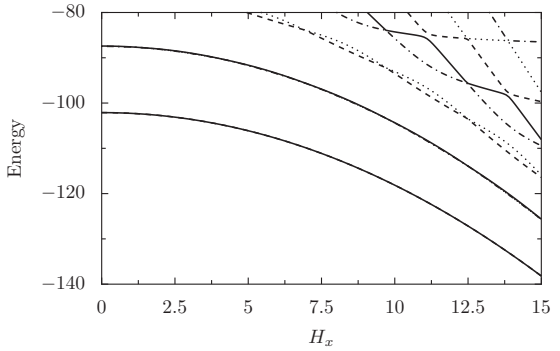

FIG. 4. Energy diagram of the low-lying levels of the system (2) with $S=10$ and $E=0.3$ as functions of the field H_x. The lowest energy and the first-excited energy almost degenerate in this vertical axis scale. The second-excited energy and the third-excited energy are also almost degenerate.

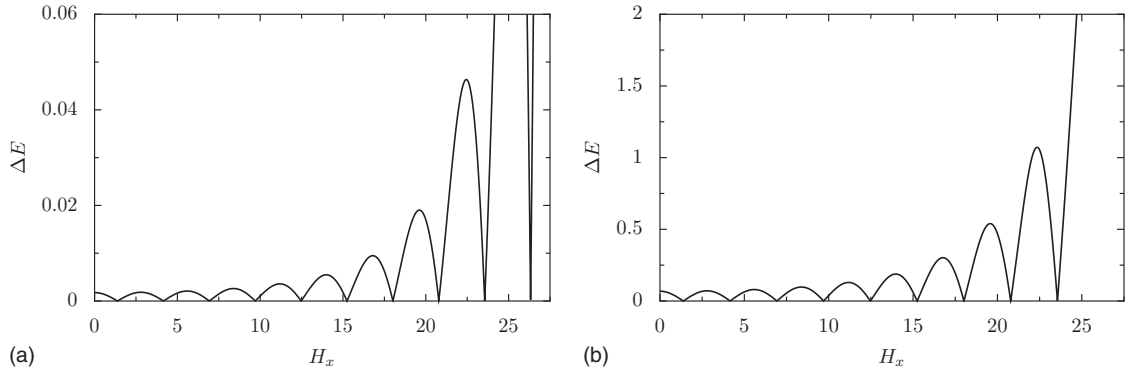

FIG. 5. (a) Energy gap between the lowest energy and the first-excited energy for $E=0.3$ as a function of the field H_x. There are ten diabolical points. (b) Energy gap between the second-excited energy and the third-excited energy for $E=0.3$. In this case, there are nine diabolical points.

There, the energy gap ΔE has a shape which has often appeared in literature (Fig. 5).

IV. EFFECTS OF A HIGHER-ORDER ANISOTROPY

In single molecular magnets with large spins, e.g., Mn_{12} (Refs. 45–47) and Fe_8,[18] the existence of the higher-order anisotropic term,

$$\mathcal{H}'' = C(S_+^4 + S_-^4) \tag{15}$$

has been suggested. In this section, we study effects of this fourth-order anisotropy. The Hamiltonian without the magnetic field is

$$\mathcal{H} = -DS_z^2 + E(S_+^2 + S_-^2) + \mathcal{H}''. \tag{16}$$

Here it should be noted as follows. Because $S_+ = S_x + iS_y$ and $S_- = S_x - iS_y$, and

$$S_+^4 + S_-^4 = 2S_x^4 + 2S_y^4 - 6S_x^2S_y^2 - 6S_y^2S_x^2 - 4i(S_xS_zS_y - S_yS_zS_x) - 2S_z^2. \tag{17}$$

Thus, in the representation which diagonalize M_x, i.e., $\{|M_x\rangle\}$, it is given by

$$S_+^4 + S_-^4 = 2S_x^4 + \frac{1}{8}(S_x^+ + S_x^-)^4 - \frac{3}{2}S_x^2(S_x^+ + S_x^-)^2 - \frac{3}{2}(S_x^+ + S_x^-)^2S_x^2 + S_x(S_x^+ - S_x^-)(S_x^+ + S_x^-) - (S_x^+ + S_x^-)(S_x^+ - S_x^-)S_x + \frac{1}{2}(S_x^+ - S_x^-)^2, \tag{18}$$

which can change the value of M_x by multiples of 2.

Therefore, nonzero components of matrix elements of the fourth term are

$$\langle M_x = m|\mathcal{H}''|M_x = m\rangle,$$

$$\langle M_x = m|\mathcal{H}''|M_x = m \pm 2\rangle, \tag{19}$$

and

$$\langle M_x = m|\mathcal{H}''|M_x = m \pm 4\rangle.$$

Because

$$\langle M_x = m|\mathcal{H}''|M_x = m \pm 1\rangle = 0, \tag{20}$$

the fact that the gap opens only at crossing points where the magnetization M_x differs by two maintains.

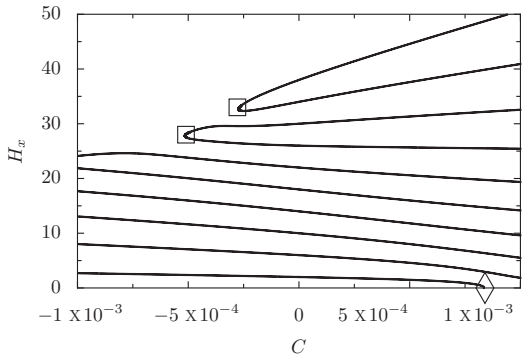

FIG. 6. Diabolical points between the lowest-energy level and the first-excited energy level on the (C, H_x) plane for the $E=0.5$. The symbol (□) denotes the type I annihilation points. The symbol (◇) denotes the type II annihilation points.

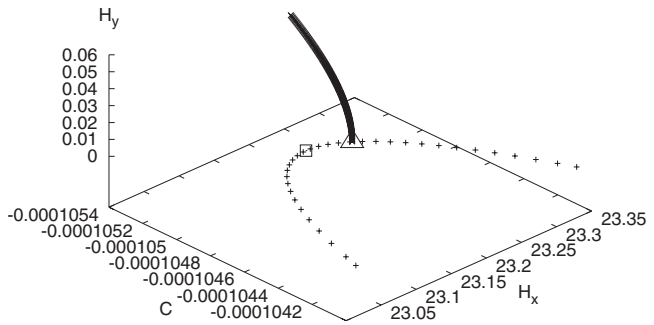

FIG. 7. The branch of diabolical points between the lowest energy and first-excited energy with largest H_x in the case of $S=10$ and $E=0.3$. The symbol (△) denotes the bifurcation point. The symbol (□) denotes the annihilation point.

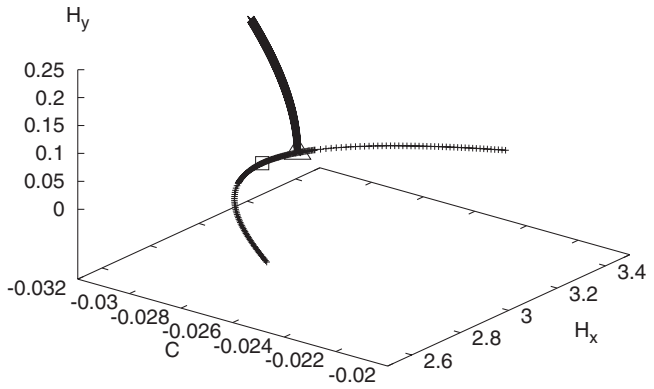

FIG. 8. The branch of diabolical points between the lowest energy and first-excited energy with largest H_x in the case of $S=2$ and $E=0.3$. The symbol (△) denotes the bifurcation point. The symbol (□) denotes the annihilation point.

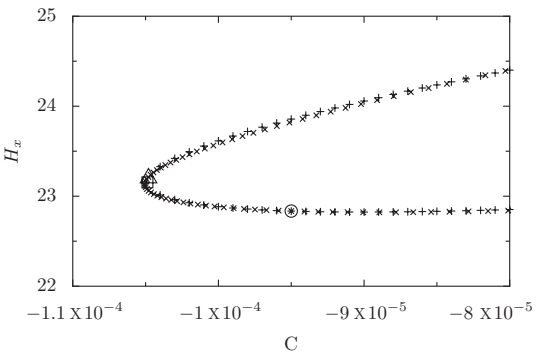

FIG. 9. Fitting of diabolical points using a rotated parabola function. The symbols (+) denote the bare numerical results for the diabolical points. The symbol (△) denotes the bifurcation point. The symbol (□) denotes the annihilation point. The symbols (×) denote points on a rotated parabola obtained by fitting, and the symbol (○) denotes the origin of the fitted parabola. (Because the scales of axes of H_x and C are different, the point denoted by the circle does not look like the origin.)

A. Dependence on C at fixed E

First let us study the behavior of the diabolical points on C at fixed value of E. We plot the change in the diabolical points in a coordinate (C,H_x) in Fig. 6. As far as $|C|$ is small, the number of diabolical points is the same as that of $C=0$. However, for large $|C|$ cases, pairs of diabolical points disappear from the figure. We call this point (C,H_x) "type I annihilation point" which is shown by (□) in Fig. 6. The pair annihilation occurs from the side of large H_x when C decreases in the negative C region. In the positive side, diabolical points are drawn into the H_x axis sequentially. At the H_x axis, the diabolical point combines with that from the negative H_x side and disappears, which we call "type II annihilation points," and denote it by (◇) in Fig. 6. At these annihilation points, the diabolical points move to a nonzero H_y region.

First, we show the motion of diabolical points around the type I annihilation point. In Fig. 7, we plot the motion of diabolical points in the largest H_x values in a $H_x>0$ subspace. There, we find that a pair of diabolical points is created in nonzero H_y region at a point. We denote this point by the symbol (△). We call this point "a bifurcation point." Here, it should be noted that the point of the creation of the pair is not the point of the annihilation of the pair on the (C,H_x) plane. We find that this separation of the annihilation point and the bifurcation point exists in all the finite values of S. In Fig. 8, we show the case of $S=2$, where we find the same type of structure. The separation is much larger than the case of $S=10$.

The effect of the fourth-order anisotropy has been discussed by Bruno.[43] His argument is the following. There is a critical value of $C=C_c$ where two diabolical points collide and at this point the bifurcation takes place. That is, a pair of two diabolical points appears at the type I annihilation point. However, we find that the bifurcation point is different from the annihilation point and appears at a larger value (smaller $|C|$) of C. This means that the number of diabolical points is not preserved on the (H_x,H_y) plane when we change C. This fact is different from Bruno's argument. In his arguments, the number of diabolical points on the (H_x,H_y) plane is preserved except at C_c. On the other hand, our numerical result shows that the number of diabolical points on the (H_x,H_y) plane can change with the value of C. Bruno's discussion is based on the large S limit. Thus, we study S dependence of the separation of the annihilation and bifurcation points.

Here, we investigate structure of the diabolical points near annihilation points. In Fig. 6, a pair of diabolical points near annihilation points has a parabolalike structure on the (C,H_x) plane. Thus, we try to fit the curve using a rotated parabola function $(a^2C^2+2abH_xC+b^2H_x^2+cC+dH_x+e=0)$ with con-

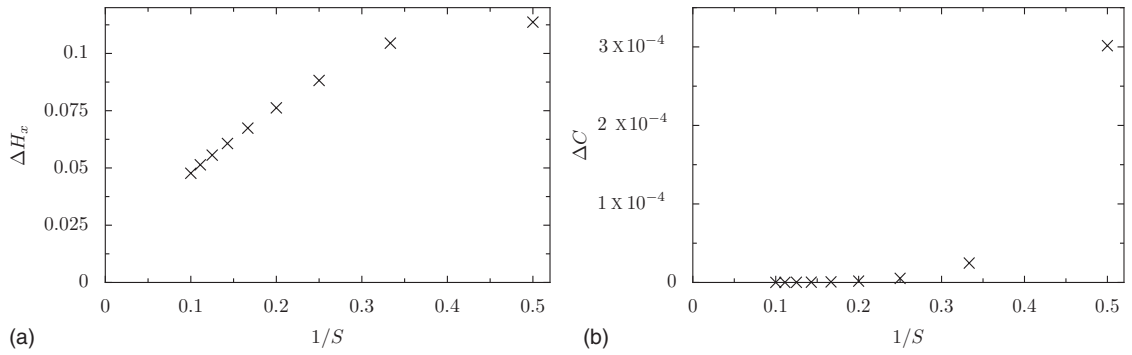

FIG. 10. (a) ΔH_x as a function of $1/S$ with $E=0.3$. (b) ΔC as a function of $1/S$ with $E=0.3$.

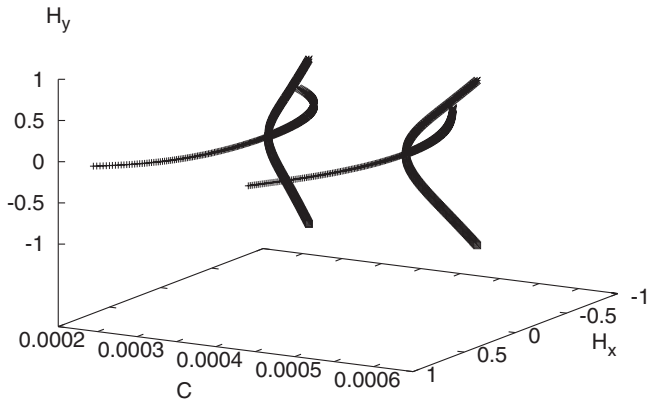

FIG. 11. Diabolical points between the lowest-energy level and the first-excited energy level on the (H_x, C, H_y) space in the case of $E=0.3$.

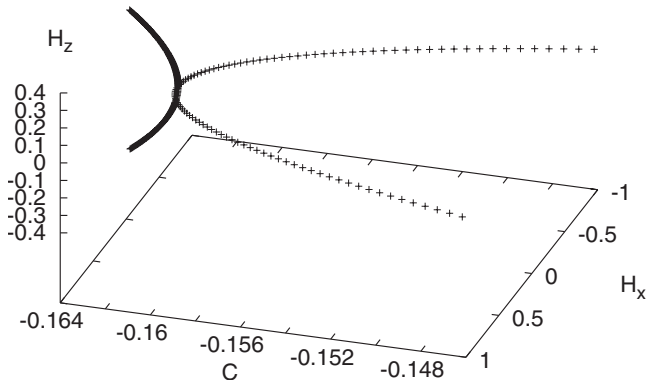

FIG. 13. Diabolical points on (H_x, C, H_z) space with $E=0.3$. for $S=3$ case.

stants (a,b,c,d,e). The fitting is given in Fig. 9. The origin of this rotated parabola where the diabolical point is located at $(C,H_x) \sim (-0.000\,095, 22.834\,68)$, which is indicated (○). The point is not the annihilation point and it is not the bifurcation point neither. This fact indicates that the bifurcation does not occur at the origin of the parabola which is a special point of this figure.

Now, we study S dependence of the distance between the bifurcation point and the annihilation point. We define two quantities,

$$\Delta C \equiv C_{\mathrm{bif}} - C_{\mathrm{ann}}, \tag{21}$$

and

$$\Delta H_x \equiv H_{\mathrm{bif}}^x - H_{\mathrm{ann}}^x, \tag{22}$$

where C_{bif} and H_{bif}^x are values of bifurcation points, and C_{ann} and H_{ann}^x are values of annihilation points.

We plot ΔC and ΔH_x as functions of $1/S$ in Fig. 10. In these figures, we find that both ΔC and ΔH_x rapidly decrease, when we increase S. Thus, our numerical results are consistent with Bruno's arguments in the large S limit. But, it should be noted that at finite values of S the bifurcation point and the annihilation point do not coincide, which indicates that there exists a nontrivial quantum effect.

Next, we show the motion of the diabolical points around the type II annihilation points. There, two diabolical points move from $(C,H_x,H_y=0)$ to $(C,H_x,H_y\neq 0)$. In Fig. 11, we show this motion of diabolical points in the (C,H_x,H_y) space.

As we saw above, the diabolical points disappear from the (C,H_x) plane by the pair annihilation. In the case that S is an odd integer, there is an odd number of diabolical points in the $H_x(>0)$ region of the (C,H_x) plane. There, the last one does not have a partner. We study how the last point behaves in the (C,H_x) plane. In Fig. 12, we show behavior of diabolical points of the model of $S=3$ in the (C,H_x) plane. In this case, there are three diabolical points in the region of $H_x>0$. In Fig. 12(a), we find the pair annihilates around $C \sim -0.003\,9$. There, the H_x value of the last point increases when C decreases. However, when C decreases further, it goes down and finally it merges to the C axis as shown in Fig. 12(b) and merges with the partner coming from the $H_x<0$ region. We call this point "the type III annihilation point." Interestingly in this case the diabolical points move to a nonzero H_z region $[C,H_x(=0),H_y(=0),H_z(\neq 0)]$ but not a nonzero H_y region $[C,H_x(\neq 0),H_y(\neq 0),H_z(=0)]$ as in the other cases. We depict this behavior of diabolical points in Fig. 13.

In this way, all the diabolical points disappear from the (C,H_x) plane when $|C|$ becomes large and found three types of annihilation points. By the above studies, we figured

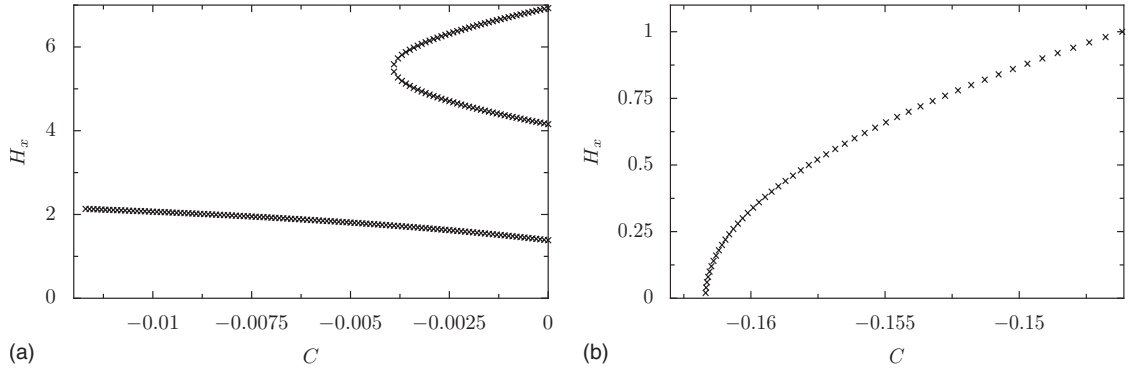

FIG. 12. Behavior of diabolical points on the (H_x, C) plane with $E=0.3$ for $S=3$ case: (a) around the last pair annihilates and (b) the last one merges to the C axis $(H_x=0)$.

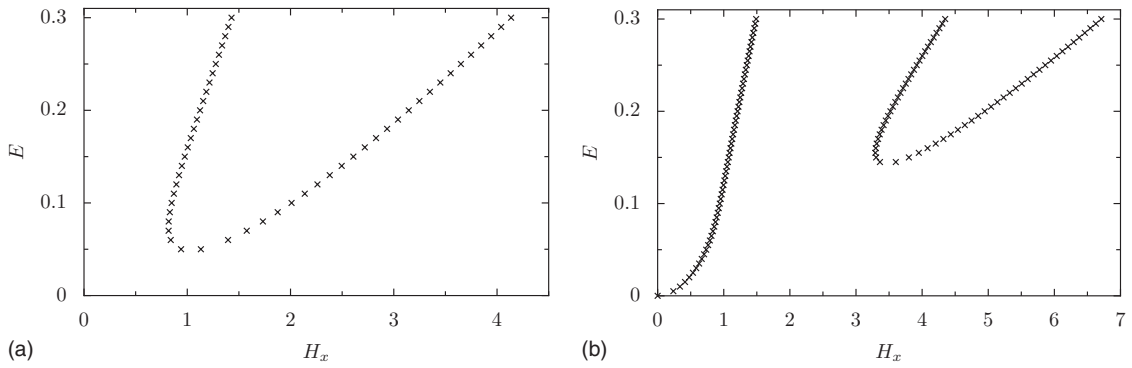

FIG. 14. Diabolical points on the (H_x,E) plane with $C=-0.001$. (a) $S=2$ and (b) $S=3$.

out complete structure of diabolical points in the (C,H_x) plane.

B. Dependence on E at fixed C

So far, we studied the behavior in the (C,H_x) plane. Here let us study E dependence of the diabolical points. In Fig. 14, we show diabolical points on the (H_x,E) plane for a fixed $C(=-0.001)$. In Fig. 14(a), we show the case of $S=2$, where the two diabolical points combine and annihilate when E becomes small. This is a type I annihilation point. There, they move to nonzero H_y region. In the case of $S=3$ cases, the last one diabolical point moves to the origin $(H_x,E)=(0,0)$ as depicted in Fig. 14(b). This is a special case of the type III annihilation point.

The same type behavior is found in larger spin cases $(S=4,5,\ldots)$ (not shown). This observation indicates that the ground state for $E=0$ is twofold degenerate in the odd spin cases. This is a degeneracy not related to Kramer's degeneracy because S is integer. We can easily understand this degeneracy. For $E=0$, a Hamiltonian is described by

$$\mathcal{H} = -DS_z^2 + C(S_+^4 + S_-^4). \tag{23}$$

If we set $C=0$, $|M_z=-S\rangle$ and $|M_z=S\rangle$ give the twofold-degenerate ground state, where $S_z|M_z\rangle=M_z|M_z\rangle$. For even spin cases, matrix element between the states $|M_z=\pm S\rangle$ is nonzero,

$$\langle M_z = S|(S_+^4 + S_-^4)^n|M_z = -S\rangle \neq 0, \tag{24}$$

because the difference of the magnetization M_z $(=2S)$ is a multiple of 4, where n is an arbitrary integer. On the other hand and for odd spin cases, the difference $2S$ is not a multiple of 4. Thus,

$$\langle M_z = S|(S_+^4 + S_-^4)^n|M_z = -S\rangle = 0. \tag{25}$$

Therefore, quantum tunneling between the two states does not occur, and the ground state is twofold degenerate in odd spin models for $E=0$ and $C\neq 0$ cases.

V. SUMMARY

We investigated nontrivial degeneracy of eigenenergies of single molecular magnets using the large single-spin model. In the parameter space (E,C,H_x,H_y,H_z), positions of the points at which the eigenenergies are degenerate (diabolical points) are studied. As has been pointed out, the model (1) has diabolical points at nonzero H_x. This fact seems nontrivial and has been studied in terms of the Berry phase in the path-integral formulation.[36] We pointed out that the existence of diabolical points at nonzero H_x is understood from a viewpoint of the parity effect of the magnetization in the x direction.

We also studied effects of the higher-order anisotropy C. For a small value of $|C|$, there are S diabolical points with positive values of H_x. We studied behavior of those points when $|C|$ increases. They move out from the (C,H_x) plane by pair annihilations. We found three types of annihilations. In the positive C case, each diabolical point moves to the C axis and at the C axis it combines with the partner coming from negative H_x region and they move to the nonzero H_y region. In the negative C case, the diabolical points make a pair with neighbors in the positive H_x region. We also found a pair creation of diabolical points in the nonzero H_y region. We should make emphasis that the annihilation points do not coincide with the creation (bifurcation) points for finite values of S. This is in contrast to the case of $S\to\infty$, which was studied by Bruno.[43] The asymptotic behavior in the limit $S\to\infty$ was studied and we found that the distance between the annihilation and the bifurcation points decreases to zero when S increases. Thus, the argument of semiclassical picture is valid, but there exists an intrinsic quantum effect. In the case of odd integer S, one diabolical point remains unpaired and it moves to the C axis and makes pair with a partner coming from negative H_x. In this case, we found that they move to the nonzero H_z region.

ACKNOWLEDGMENTS

The authors thank Keiji Saito for fruitful discussions. The present work was supported by Grant-in-Aid for Scientific Research on Priority Areas, and also the Next Generation Super Computer Project, Nanoscience Program from MEXT of Japan. The numerical calculations were supported by the supercomputer center of ISSP of Tokyo University.

[1] D. Gatteschi, R. Sessoli, and J. Villain, *Molecular Nanomagnets* (Oxford University Press, New York, 2006).
[2] W. Wernsdorfer, Adv. Chem. Phys. **118**, 99 (2001).
[3] D. Gatteschi and R. Sessoli, Angew. Chem., Int. Ed. **42**, 268 (2003).
[4] S. J. Blundell and F. L. Pratt, J. Phys.: Condens. Matter **16**, R771 (2004).
[5] E. del Barco, A. D. Kent, S. Hill, J. M. North, N. S. Dalal, E. M. Rumberger, D. N. Hendrickson, N. Chakov, and G. Christou, J. Low Temp. Phys. **140**, 119 (2005).
[6] B. Barbara, L. Thomas, F. Lionti, I. Chiorescu, and A. Sulpice, J. Magn. Magn. Mater. **200**, 167 (1999).
[7] L. Thomas, F. Lionti, R. Ballou, D. Gatteschi, R. Sessoli, and B. Barbara, Nature (London) **383**, 145 (1996).
[8] J. R. Friedman, M. P. Sarachik, J. Tejada, and R. Ziolo, Phys. Rev. Lett. **76**, 3830 (1996).
[9] C. Sangregorio, T. Ohm, C. Paulsen, R. Sessoli, and D. Gatteschi, Phys. Rev. Lett. **78**, 4645 (1997).
[10] J. A. A. J. Perenboom, J. S. Brooks, S. Hill, T. Hathaway, and N. S. Dalal, Phys. Rev. B **58**, 330 (1998).
[11] T. Kubo, T. Goto, T. Koshiba, K. Takeda, and K. Awaga, Phys. Rev. B **65**, 224425 (2002).
[12] L. D. Landau, Phys. Z. Sowjetunion **2**, 46 (1932).
[13] C. Zener, Proc. R. Soc. London, Ser. A **137**, 696 (1932).
[14] E. C. G. Stueckelberg, Helv. Phys. Acta **5**, 369 (1932).
[15] S. Miyashita, J. Phys. Soc. Jpn. **64**, 3207 (1995).
[16] I. Rousochatzakis, Y. Ajiro, H. Mitamura, P. Kögerler, and M. Luban, Phys. Rev. Lett. **94**, 147204 (2005).
[17] M. Ueda, S. Maegawa, and S. Kitagawa, Phys. Rev. B **66**, 073309 (2002).
[18] W. Wernsdorfer and R. Sessoli, Science **284**, 133 (1999).
[19] K. Saito and S. Miyashita, J. Phys. Soc. Jpn. **70**, 3385 (2001).
[20] I. Chiorescu, W. Wernsdorfer, A. Müller, H. Bögge, and B. Barbara, Phys. Rev. Lett. **84**, 3454 (2000).
[21] K. Saito, S. Miyashita, and H. De Raedt, Phys. Rev. B **60**, 14553 (1999).
[22] S. Bertaina, S. Gambarelli, T. Mitra, B. Tsukerblat, A. Müller, and B. Barbara, Nature (London) **453**, 203 (2008).
[23] K.-Y. Choi, Y. H. Matsuda, H. Nojiri, U. Kortz, F. Hussain, A. C. Stowe, C. Ramsey, and N. S. Dalal, Phys. Rev. Lett. **96**, 107202 (2006).
[24] M. N. Leuenberger and D. Loss, Nature (London) **410**, 789 (2001).
[25] C. P. Bean and J. D. Livington, J. Appl. Phys. **30**, S120 (1959).
[26] E. M. Chudnovsky, Sov. Phys. JETP **50**, 1035 (1979).
[27] U. Weiss and W. Haeffner, Phys. Rev. D **27**, 2916 (1983).
[28] S. Coleman, *Aspects of Symmetry* (Cambridge University Press, Cambridge, 1985).
[29] R. Rajaraman, *Solitons and Instantons: An Introduction to Solitons and Instantons in Quantum Field Theory* (North-Holland, Amsterdam, 1987).
[30] E. N. Bogachek and I. V. Krive, Phys. Rev. B **46**, 14559 (1992).
[31] M. V. Berry and M. Wilkinson, Proc. R. Soc. London, Ser. A **392**, 15 (1984).
[32] M. V. Berry, Proc. R. Soc. London, Ser. A **392**, 45 (1984).
[33] D. Loss, D. P. DiVincenzo, and G. Grinstein, Phys. Rev. Lett. **69**, 3232 (1992).
[34] J. von Delft and C. L. Henley, Phys. Rev. Lett. **69**, 3236 (1992).
[35] E. M. Chudnovsky and D. P. DiVincenzo, Phys. Rev. B **48**, 10548 (1993).
[36] A. Garg, Europhys. Lett. **22**, 205 (1993).
[37] A. Garg, E. Kochetov, K.-S. Park, and M. Stone, J. Math. Phys. **44**, 48 (2003).
[38] J. Villain and A. Fort, Eur. Phys. J. B **17**, 69 (2000).
[39] E. Keçecioğlu and A. Garg, Phys. Rev. B **63**, 064422 (2001).
[40] A.-L. Barra, P. Debrunner, D. Gatteschi, C. H. E. Schulz, and R. Sessoli, Europhys. Lett. **35**, 133 (1996).
[41] E. Keçecioğlu and A. Garg, Phys. Rev. Lett. **88**, 237205 (2002).
[42] E. Keçecioğlu and A. Garg, Phys. Rev. B **67**, 054406 (2003).
[43] P. Bruno, Phys. Rev. Lett. **96**, 117208 (2006).
[44] A. Caneschi, D. Gatteschi, and R. Sessoli, J. Am. Chem. Soc. **113**, 5873 (1991).
[45] I. Mirebeau, M. Hennion, H. Casalta, H. Andres, H. U. Güdel, A. V. Irodova, and A. Caneschi, Phys. Rev. Lett. **83**, 628 (1999).
[46] S. Hill, J. A. A. J. Perenboom, N. S. Dalal, T. Hathaway, T. Stalcup, and J. S. Brooks, Phys. Rev. Lett. **80**, 2453 (1998).
[47] A. L. Barra, D. Gatteschi, and R. Sessoli, Phys. Rev. B **56**, 8192 (1997).